International Journal of Civil Engineering

Structural Engineering

# Corrosion detection of reinforced concrete beams with wavelet analysis

**R. Abbasnia*, A. Farsaei**

Received: May 2012, Revised: November 2012, Accepted: June 2013

***Abstract***

*Corrosion of reinforcing steel and other embedded metals is the main cause of severe deterioration in reinforced concrete members which subsequently imposes adverse effects on ultimate and serviceability limit state performance of the whole structure. In this paper, a new corrosion detection method for reinforced concrete beams, based on wavelet analysis is presented. To evaluate the capability and efficiency of the method, a simply supported RC beam is modeled in 3-D taking into account the behaviors of concrete, steel and bond degradation. Deflection profile and mode shapes are extracted numerically and analyzed by wavelet transform. Based on the numerical results obtained, it can be concluded that this wavelet-based method is capable of detecting corrosion at its earliest stage. It is also concluded that both discrete and continuous wavelet transforms can be used and mother wavelet type has no significant effect on the results.*

***Keywords:*** *Wavelet transform, Damage identification, Non destructive test.*

## 1. Introduction

In recent years, the field of structural health monitoring (SHM) has been the subject of intensive investigation because of its feasibility and practical importance in damage detection [1,2,3]. The main purpose in SHM is to detect damage at its earliest possible stage to prevent severe deterioration and reduce subsequent repair costs. SHM has been used successfully in mechanical, aerospace, and civil engineering structures. To obtain the best results in conventional damage detection methods such as ultrasonic pulse waves, schmidt rebound hammer and half-cell potential which are visual and localized methods, location of damage should be primarily accessible and determined by an in situ inspection. To overcome this limitation, there has been an emerging trend towards the use of vibration characteristics of structures to detect damage. The basic concept of this method is that modal parameters (notably: natural frequencies, mode shapes and modal damping) are functions of physical and mechanical properties of the structures (mass, damping and stiffness). Therefore, changes in these properties will cause changes in modal parameters [4].

One of the dynamic properties which has been used by many researchers is, shift in natural frequencies. In this method, the real modal frequency of the existing structure is obtained by special equipment in situ and then it is compared with mathematically predicted frequency of intact structure. Shifts in modal frequency prove the existence of damage but no more information about the location and severity of damage can be extracted. Tests conducted on I-40 Bridge [2] demonstrated that severe damage in a localized section of the bridge causes a minor shift in modal frequency. In fact, modal frequencies are related to global properties and do not provide any information regarding local changes in structural characteristics.

Mode shape is another dynamic property which has been used by researchers in the field of health monitoring and damage detection [5]. West [6] was probably the first who used the concept of mode shapes to predict the location of damage in structures. Pandey et al. [7] presented a method which uses mode shape curvature as an indicator of damage for evaluation of damaged and undamaged structures. It should be noted that most of these methods need a baseline obtained from the undamaged structure which is the main deficiency, since in most of the practical cases only the properties of damaged structure are available.

One of the first attempts for detecting structural damage without baseline information is gapped smoothing method propounded by Ratclif et al. [3]. Wavelet analysis is an efficient tool in signal processing and has recently been used in the

* *Corresponding Author: abbasnia@iust.ac.ir*
*Civil engineering department, Iran University of science and Technology, Tehran, Iran*

damage detection. Staszewski [8] presents a summary of recent advances and applications of wavelet analysis for damage detection. Kijewski and Kareem [9] evaluated the feasibility and practicality of wavelet analysis for damage detection and identification of a structure in civil engineering. Continuous and discrete wavelet analysis are mostly used in the field of structural health monitoring. The main advantage of the continuous wavelet transform (CWT) is its ability to elucidate real-time information in time (or space) and scale (or frequency) with adaptive windows. An application of wavelet theory in spatial domain is detection of crack in structures which was proposed by Liew and Wang [10]. The crack location is indicated by a peak in the profile of the wavelets coefficients along the length of the beam. Wang and Deng, 1999 [11] proposed that the wavelet transform can be directly applied to spatially distributed structural response signals, such as surface profile, displacement, strain or acceleration measurements. Several studies used CWT of the fundamental mode shape exponent to detect the location and extent of damage in a beam Hong et al. [12] , Gentile and Messina [13], Douka et al.[14] and Wu and Wang [15] .

Reinforcement corrosion in RC structures is an electro chemical reaction which can cause severe reduction in serviceability and ultimate capacity of the structures. Corrosion products cause extensive volumetric expansion and therefore lead to splitting in concrete and meanwhile reduce reinforcement cross sectional area and bonding strength. Although corrosion causes severe damages in structures particularly bridges, using corrosion detection techniques based on health monitoring approaches can efficiently prevent these damages. Therefore, the present study aims to develop a new corrosion detection method based on wavelet analysis to detect early stage corrosion without baseline information. Discrete and continuous wavelet transforms with Minimum number of vanishing moments are used in this study.

## 2. Application of wavelet transform in damage detection

Wavelet transform is a powerful tool for image and signal processing as well as generation of artificial ground motion records [16]. In recent years, some studies have proven the efficacy of this theory as a damage detection and localization tool (e.g. [11-15]). Wavelet transform has the ability to detect fluctuations in a signal and therefore can be used to detect fluctuations in a damaged structure profile like mode shape or its derivatives. In this section, application of continuous and discrete wavelet transform in damage detection is presented, respectively.

### *2.1. Continuous Wavelet Transform (CWT)*

A wavelet is an oscillatory, real- or complex-valued function $\psi(x) \in L^2(R)$.This function has zero average and finite length. Function $\psi(x)$ is a mother wavelet and $L^2(R)$ denotes the Hilbert space function which is measurable, square-integrable and one-dimensional [17]. This function is used to create a family of wavelets as follows:

$$\psi_{u,s}(x) = \frac{1}{\sqrt{s}}\psi\left(\frac{x-u}{s}\right) \tag{1}$$

where, $u$ and $s$ are real translation and dilation parameters, respectively. Translation parameter determines the location of wavelet window along the space axis and dilation parameter represents the width of wavelet window. Therefore, in contradiction to Fourier transform method, information related to space and frequency is recorded simultaneously. Therefore, CWT for a given signal $f(x)$ is defined as in (Eq. 2):

$$Wf(u,s) = \frac{1}{\sqrt{s}}\int_{-\infty}^{+\infty} f(x)\psi\left(\frac{x-u}{s}\right) \tag{2}$$

where $Wf(u,s)$ defines the wavelet coefficient of a given signal and it varies between 0 and 1. This coefficient determines the level of similarity between signal and corresponding wavelet function at the vicinity of the point u with scale s. Value 1 denotes the absolute similarity (presence of fluctuations in signal) and value 0 (signal is smooth at vicinity of point $u$) represents no similarity. Therefore, a peak or sudden change in wavelet coefficient can show the presence of fluctuations in response to the damaged structure.

It should be noted that application of wavelet transforms with appropriate number of vanishing moments plays an important role in detection of signal singularities. A wavelet with n vanishing moments should satisfy Eq. (3):

$$\int_{-\infty}^{+\infty} x^k \psi(x)d(x) = 0 \quad , k = 0,1,2,3,...,n-1 \tag{3}$$

Wavelet with $n$ vanishing moments ensures zero or very small value for wavelet coefficient because it is orthogonal to polynomials up to $n$-$1$ degree. In the case of mode shapes which are similar to polynomial degree 4 wavelets with at least 4 vanishing moments is required for a robust damage detection procedure.

### *2.2. Discrete Wavelet Transform (DWT)*

In practical signal processing, a discrete version of wavelet transform is mostly employed by choosing discrete dilation parameter s and the translation parameter u [18]. In fact, continuous transform includes redundant information which is not required for signal processing. In general, the procedure becomes much more efficient and the computational efforts will be greatly reduced if dyadic values of u and s are used as follows:

$$s = 2^j \quad , u = 2^j k \qquad j,k \in Z \tag{4}$$

where $Z$ is the set of positive integers and the corresponding discrete wavelet function is written as in (Eq. 5):

$$\psi_{j,k}(x) = 2^{\frac{j}{2}}\psi\left(2^j x - k\right) \tag{5}$$

Wavelet expansion function ($F(x)$) and the coefficients of the wavelet expansion, $\alpha_{j,k}$ are defined according to Eq. (6) and Eq. (7):

$$F(x) = \sum_j \sum_k \alpha_{j,k}\psi_{j,k}(x) \tag{6}$$

$$\alpha_{j,k} = \int_{-\infty}^{+\infty} F(x)\overline{\psi}_{j,k}(x)d(x) \tag{7}$$

where the $\overline{\psi}_{j,k}(x)$ is the complex conjugate of the function

$\psi(x)$. Finally, using a DWT, a signal can be decomposed into its approximation and detail coefficients at the $J_{th}$-level as Eq. (8) and Eq. (9), respectively:

$$A_J = \sum_{j>J} D_J \tag{8}$$

$$D_J = \sum_{k\in Z} \alpha_{J,k}\psi_{J,k}(x) \tag{9}$$

reconstructed the two components is presented in Eq. (10):

$$F(x) = A_J + \sum_{j\le J} D_J \tag{10}$$

In the field of damage detection, the wavelet approximation coefficient conveys the intact and sound structure information, while the wavelet detail coefficient contains the information of the damage. It should be noted that this coefficient could contain the noise in the corresponding signal. Presence of a peak in detail coefficient can represent the location of a defect if there is not any noise (like wind or vehicle vibration) in the system. In the presence of noise, decomposition should be done into various levels by selecting different dyadic scales to separate the effects of noise and damage.

In this paper, the accuracy and practicality of the both CWT and DWT with suitable mother wavelets and minimum required number of vanishing moments for optimum detection of corrosion is evaluated.

## 3. Materials modeling

The applied models for concrete, reinforcing steel and steel-to-concrete bond behavior are introduced in this section. These models have the ability to take into account the corrosion effects on material degradation.

### *3.1. Concrete modeling*

The idea of coupled mechanical-environmental damage model developed by Saeta et al. [19] is used in this study to represent the concrete behavior under static as well as dynamic loading, including environmental degradation. Two different parameters of $d_t$ and $d_c$ for tension and compression damage are used as mechanical damage modifiers in the damaged plasticity model which are represented by Eq. (11) and Eq. (12):

$$\sigma_t = (1-d_t)\, E_o\, (\varepsilon_t - \tilde{\varepsilon}_t^{pl}) \tag{11}$$

$$\sigma_c = (1-d_c)\, E_o\, (\varepsilon_c - \tilde{\varepsilon}_c^{pl}) \tag{12}$$

where $E_o$ is the initial or undamaged elastic stiffness, the subscripts $t$ and $c$ refer to tensile and compression, respectively. $\tilde{\varepsilon}_t^{pl}$ and $\tilde{\varepsilon}_c^{pl}$ are the equivalent plastic strains. $\sigma_t$ and $\sigma_c$ denote tension and compressive strengths, respectively. $\varepsilon_t$ and $\varepsilon_c$ represent tension and compression strains, respectively.

Considering tension stiffening in stress-strain relation, the post failure behavior of concrete under tension (cracked concrete) and the effects of reinforcing steel-concrete interaction can be modeled easily. As discussed by [20], for reinforced concrete it is accepted to assume that tension in concrete becomes zero linearly at a total strain of about 10 times the cracking strain ($\varepsilon_{ot}^{el}$) as it is shown in Fig. 1.a.

It is also possible to model concrete behavior outside the elastic range by defining tabular data of compressive stress as a function of inelastic strain $\tilde{\varepsilon}_t^{pl}$ (Eq. (13)), as it is presented in Fig. 1b.

$$\tilde{\varepsilon}_t^{pl} = \varepsilon_c - \varepsilon_{ot}^{el} \tag{13}$$

where

$$\varepsilon_{oc}^{el} = \frac{\sigma_{co}}{E_o} \tag{14}$$

and $\sigma_{co}$ denotes maximum compressive stress within the elastic zone.

A yield function proposed by Lubliner et al. [20] is employed to account for different evolutions of strength under tension and compression. In terms of effective stresses the yield function takes the mathematical form of (Eq. 15):

$$F(\bar{\sigma},\tilde{\varepsilon}^{PL}) = \frac{1}{1-\alpha}(\bar{q} - 3\alpha\bar{p} + \beta(\tilde{\varepsilon}^{PL}) < \hat{\bar{\sigma}}_{\max} > -\gamma < -\hat{\bar{\sigma}}_{\max} >) - \bar{\sigma}_c(\tilde{\varepsilon}^{PL}) \tag{15}$$

where $\alpha$ and $\beta$ are dimensionless material constants; $\bar{p}$ is the effective hydrostatic pressure; $\bar{q}$ is the Mises equivalent effective stress; $\bar{s}$ is the deviatoric part of the effective stress tensor and $\hat{\bar{\sigma}}_{max}$ is the algebraically maximum eigenvalue of $\bar{\sigma}$ and the parameter $\gamma$ takes the value of 3 [20].

The flow potential G chosen for this model is the Drucker-Prager hyperbolic function as (Eq. 16):

$$G = \sqrt{(\epsilon\, \sigma_{to}\tan\psi)^2 + \bar{q}^2} - \bar{p}\tan\psi \tag{16}$$

where $\psi$ is the dilation angle measured in the $p$–$q$ plane at high confining pressure; $\sigma_{to}$ is the uniaxial tensile stress at

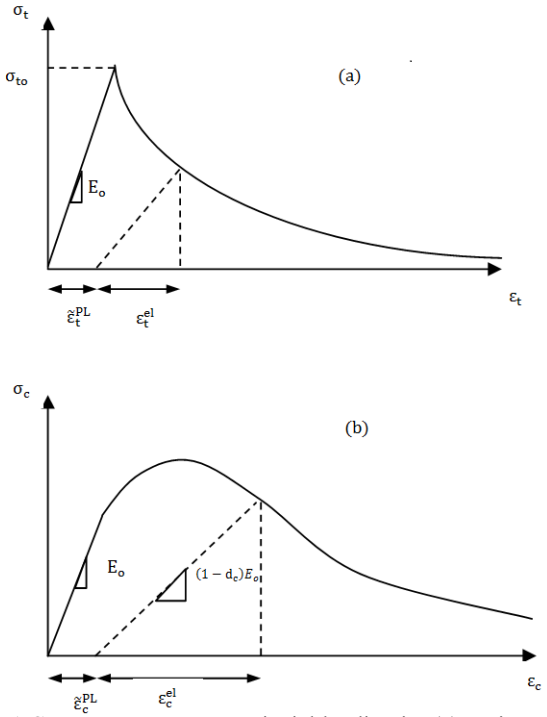


**Fig. 1** Concrete response to uniaxial loading in: (a)tension and (b)compression [19].

failure; and $\varepsilon$ is a parameter, referred to as the eccentricity, which defines the rate at which the function approaches the asymptote (the flow potential tends to a straight line as the eccentricity tends to zero). This flow potential, which is continuous and smooth, ensures that the flow direction is defined uniquely.

To account for the mechanical effects of corrosion in concrete structures, a coupled chemical–mechanical damage model has been developed, by introducing an additional internal variable, called 'environmental damage dchem in the stress-strain relationship (similar to the approach proposed in [19] and [21]). Substituting this variable into the Eqs. (11 and 12), they can be re-written as follows:

$$\sigma_t=(1-d_{chem})(1-d_t)\,E_o\,(\varepsilon_t-\tilde{\varepsilon}_t^{pl}) \tag{11}$$

$$\sigma_c=(1-d_{chem})(1-d_c)\,E_o\,(\varepsilon_c-\tilde{\varepsilon}_c^{pl}) \tag{12}$$

The environmental damage parameter $d_{chem}$ is a function of development level of the chemical reaction and the relative residual strength of the material [19]. The environmental damage parameter is presented by an increasing function of time. It should be noted that this damage parameter has the same effect in tension or compression.

### *3.2. Reinforcement modeling*

Within the framework of finite element method, to model the reinforcing steel in concrete, two different approaches can be used: "smeared approach" in which steel is smeared into a layer between concrete layers; the second one is called "detailed approach" in which steel and concrete are modeled as distinct elements. The first method, which is frequently used for analyzing the global behavior of RC structural elements, is not directly applicable when the corrosion phenomenon is considered. Actually such an approach cannot easily simulate the loss of bond between steel and concrete, which is a fundamental issue in corrosion problems. Among different possibilities allowed by the "detailed approach", an elastic constitutive relationship with isotropic hardening has been adopted for reinforcing steel.

A linear elastic material model is used to model reinforced concrete. The total stress is defined from the total elastic strain as follows (Eq. 19):

$$\sigma = D^{el}\,\varepsilon^{el} \tag{19}$$

where $\sigma$ is the total stress, or Cauchy (true) stress in finite-strain problems, $D^{el}$ is the fourth-order elasticity tensor, and $\varepsilon^{el}$ represents the total elastic strain.

As discussed in [21], corrosion effects on cross sectional area and ductility of reinforcement are both considered and reduction in yield and ultimate strength are neglected. Reduction in cross section is applied based on equation proposed by Berto et al. [22] as follows:

$$A_s = \frac{N_S\,\pi\,[D_o-nx]^2}{4} \tag{20}$$

where $N_s$ is the number of steel bars of the same diameter, $D_0$ is the original diameter of steel bars, $n$ takes into account the possibility of a one-sided or two-sided corrosion attack and $x$ is the corrosion depth in the reinforcement.

In this phase of the research, the effect of corrosion on steel bar ductility is introduced in the model by adopting the approach recently proposed by [22]. According to this approach the steel ultimate strain $\varepsilon'_{su}$ can be considered as linearly dependent on the reduction of the bar cross-section, by defining $\alpha_{pit}$ as (Eq. 21):

$$\alpha_{pit}=\frac{\Delta A_{pit}}{A_{rebar}} \tag{21}$$

where $\Delta A_{pit}$ is the cross sectional area reduction because of corrosion and $A_{rebar}$ is the nominal reinforcement cross-section, Therefore $\varepsilon'_{su}$ can be presented by (Eq. 22) :

$$\varepsilon'_{su} = \left(\varepsilon_{su} - \varepsilon_{su}\right)\left(1-\frac{\alpha_{pit}}{\alpha_{pit}^{\max}}\right) \tag{22}$$

### *3.3. Bond modeling*

The bonding strength at the steel-concrete interface plays an important role in defining the behavior of RC elements, to ensure the safety level as well as the adequate structural ductility (e.g. [23]). Therefore, an efficient modeling of bond behavior is a major issue to prevent relative displacements between steel and concrete.

This model should include not only the effect of bond strength value, $\tau_{max}$ , but also definition of the shape of the bonding curve similar to concrete stress – strain relationship. Furthermore, it should consider the corrosion level. To achieve this aim, following the approach described in section 3.1 for environmental damage in concrete, a corrosion bond damage parameter, $d_{bond}$ , was introduced, similar to the variable $d_{chem}$ of Eq. (17) and defined as a monotonically increasing function of the corrosion level, with values ranging between 0 and 1. Hence, the relationship between parameters $\tau$ and $s$ can be mathematically represented by Eq. (23):

$$\tau_{max} = (1\text{-}d_{bond})G\gamma \tag{23}$$

where $G$ is the elastic shear modulus; $s$ is relative slip between concrete and reinforcement; $\gamma = s/t$ is the shear strain and $t$ is element thickness. Consequently, by adopting the unique parameter $d_{bond}$, the proposed model can describe the reduction of bond strength as well as the peak stress value corresponding to corrosion level, as illustrated in the $\tau$–$s$ curve shown in Fig. 2.

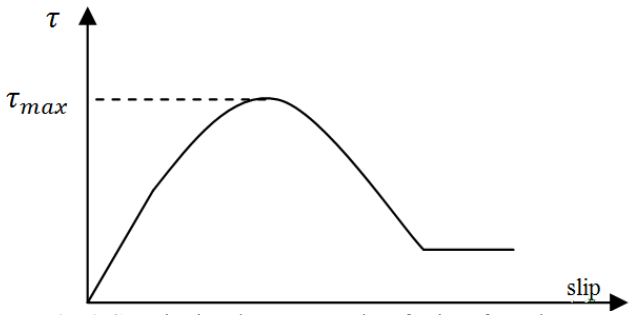


**Fig. 2** Constitutive damage type law for interface element

## 4. Numerical analysis

To assess the accuracy and the capability of the proposed method, a simply supported reinforced concrete beam of 1000 mm length and 50 mm x 100 mm cross sectional area is modeled for damage detection. To obtain Concrete Damaged Plasticity (CDP) parameters, experimental results of JANKOWIAK [24] , as summarized in Table 1, were used. Bond model parameters were obtained by experimental results provided by [22] and are shown in Table.2. Maximum value of 20 percent was considered for environmental damage parameter, $d_{chem}$ based on the findings of [22].

For the FE analysis, solid (continuum) elements with 8 integration points (CD8R), and mesh size of 5 mm is used to ensure accurate solutions. An interface layer was modeled between concrete and reinforcement elements and bonding properties were attributed to this layer.

Field investigation has proven that corrosion starts from a small part of the reinforcement and propagates to other parts gradually [22]. Therefore, this idea was used in modeling of damage with different corrosion percentages in reinforced damaged zone as shown in Fig. 3. Damaged zone was divided into 3 sub zones; i.e. the side zone, middle zone and central zone. Central, middle, and side zones were modeled with highest, moderate, and lowest corrosion levels, respectively.

In this study 15 scenarios are considered for corrosion detection as displayed in Table 3. In each case, static deflection profile of the beam under uniform load of 2.5 N/m or mode shape profile related to its free vibration is extracted numerically. Then, these profiles are analyzed by wavelet

**Table 1** The material parameters of CDP model for concrete class B50[23]

| Material's prameters | B50 | The parameters of CDP model | |
|---|---|---|---|
| | | ψ | 38 |
| | Concrete elasticity | | |
| E[GPa] | 19.7 | ϵ | 0.1 |
| ν | 0.19 | γ | 3 |
| Concrete compression hardening | | Concrete compression damage | |
| Stress [MPa] | Inelastic strain $\tilde{\varepsilon}_c^{pl}$ [-] | Damage C [-] | Inelastic strain $\tilde{\varepsilon}_c^{pl}$ [-] |
| 15 | 0 | 0 | 0 |
| 20.197804 | 0.00007473 | 0 | 0.00007473 |
| 30.000609 | 9.88479E-05 | 0 | 9.88479E-05 |
| 40.303781 | 0.000154123 | 0 | 0.000154123 |
| 50.007692 | 0.000761538 | 0 | 0.000761538 |
| 40.23609 | 0.002557559 | 0.195402 | 0.002557559 |
| 20.23609 | 0.005675431 | 0.596382 | 0.005675431 |
| 5.257557 | 0.011733119 | 0.894865 | 0.011733119 |
| Concrete tension stiffening | | Concrete tension damage | |
| Stress [MPa] | Inelastic strain $\tilde{\varepsilon}_t^{pl}$ [-] | DamageT [-] | Inelastic strain $\tilde{\varepsilon}_t^{pl}$ [-] |
| 1.99893 | 0 | 0 | 0 |
| 2.842 | 0.00003333 | 0 | 0.00003333 |
| 1.86981 | 0.000160427 | 0.406411 | 0.000160427 |
| 0.862723 | 0.000279763 | 0.69638 | 0.000279763 |
| 0.226254 | 0.000684593 | 0.920389 | 0.000684593 |
| 0.056576 | 0.00108673 | 0.980093 | 0.00108673 |

**Table 2** Corrosion effect on bond characteristics [21]

| Corrosion percentage | Shear module(Mpa) | Max. bond strength(Mpa) |
|---|---|---|
| 0 | 3350 | 16 |
| 4.27 | 2100 | 14 |
| 6.7 | 950 | 8 |
| 7.8 | 400 | 4 |

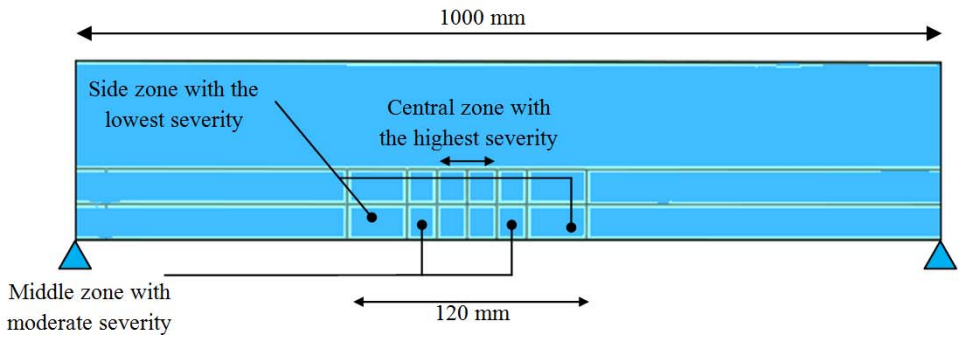


**Fig. 3** Corrosion propagation along damaged zone

**Table 3** Corrosion scenarios 1 to 15

| case no. | % corrosion Location one | | | % corrosion Location two | | | Effects considered in modeling | | |
|---|---|---|---|---|---|---|---|---|---|
| | side | middle | center | side | middle | center | concrete | reinforcement | bonding |
| 1 | - | - | - | - | - | - | - | - | - |
| 2 | 2 | 2 | 2 | - | - | - | ● | - | - |
| 3 | 2 | 2 | 2 | - | - | - | - | ● | |
| 4 | 2 | 2 | 2 | - | - | - | - | - | ● |
| 5 | 6 | 8 | 10 | - | - | - | ● | ● | ● |
| 6 | 4 | 6 | 8 | - | - | - | ● | ● | ● |
| 7 | 2 | 4 | 6 | - | - | - | ● | ● | ● |
| 8 | 1 | 2 | 4 | - | - | - | ● | ● | ● |
| 9 | 1 | 1 | 2 | - | - | - | ● | ● | ● |
| 10 | 6 | 8 | 10 | 6 | 8 | 10 | ● | ● | ● |
| 11 | 4 | 6 | 8 | 4 | 6 | 8 | ● | ● | ● |
| 12 | 2 | 4 | 6 | 2 | 4 | 6 | ● | ● | ● |
| 13 | 1 | 2 | 4 | 1 | 2 | 4 | ● | ● | ● |
| 14 | 1 | 1 | 2 | 1 | 1 | 2 | ● | ● | ● |
| 15 | 5 | 6 | 7 | - | - | - | ● | ● | ● |

transform to detect corrosion.

Scenario number 1 is defined to verify the correctness and precision of the finite element modeling by considering an undamaged simply supported beam. Concrete, steel and bonding degradation are considered individually in scenarios number 2, 3, and 4, respectively. It should be mentioned that in other damaged scenarios, these effects are considered simultaneously.

Scenarios numbers 5 to 9 were developed with single damage location and different corrosion percentage in damaged zone to investigate the effectiveness of wavelet analysis in damage detection. Then, these five scenarios are employed to define a relation between corrosion percentage and wavelet coefficient. Capability of the proposed method in detection of multiple damages is assessed with scenarios number 10 to 14 which consist of two damage locations at one third and two thirds of the beam length with the same corrosion level and damage length in each location. Finally, to verify the ability of the proposed relation in detection of corrosion severity, scenario number 15 is evaluated.

## 5. Results

In this section, the results of numerical studies are presented and discussed. At first, to verify the accuracy of the finite element modeling presented in previous section, an undamaged beam (scenario 1) is analyzed and its deflection profile as well as its first mode shape is obtained and compared with the result of basic theoretical formulations of structural mechanics [25], as shown in Figs. 4 and 5. As it can be seen

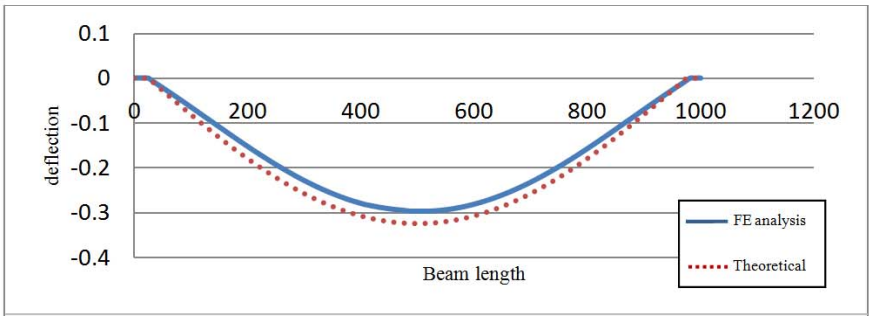


**Fig. 4** Undamaged beam static deflection profile (computed by FE analysis and theoreticalformulation)

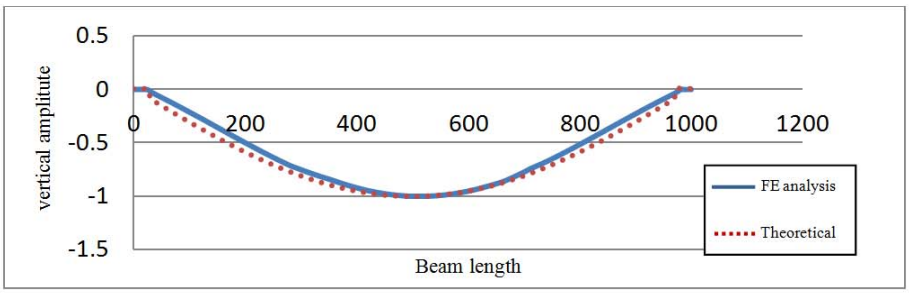


**Fig. 5** Undamaged beam first mode shape (computed by FE analysis and theoretical formulation)

from these figures, they are in good agreement with each other.

As mentioned in section 3, corrosion is modeled taking into account the role and behavior of concrete, reinforcing metal and bonding degradation. To investigate the sensitivity of this damage detection technique to these deteriorations individually, the first mode shape with respect to the scenarios numbers 2, 3, and 4 are analyzed with discrete wavelet transform and in each case, similar peaks in wavelet coefficients profile is observed. It should be noted that, scenario number 3 (taking into account only the reinforcement deterioration) had the highest peak. Therefore, corrosion can be efficiently modeled via reinforcement degradation which is possible with less computational efforts. However, to provide accurate results, corrosion is modeled in scenarios 5 to 15 taking into account all the three degradation effects simultaneously.

Corrosion propagation could be prevented if it is detected at its early stage. Therefore, static deflection profile of damaged beam with 2 percent corrosion (scenario number 9) is analyzed to demonstrate the capability of the presented method in detection of corrosion in its early stage. Continuous and discrete wavelet transforms are used in this step and the results obtained show the high efficiency in the damage detection. It can be easily seen that in the vicinity of corrosion zone, there is a peak in wavelet coefficients that can be used as an indicator for damage existence and location, as shown in Fig. 6. Therefore, it can be concluded that both CWT and DWT have the ability to detect corrosion in RC beams. However, discrete wavelet transform is used for the rest of the study because of its simplicity and reduced amount of data, it provides.

The first mode shape of the scenario number 9 is also analyzed using different mother wavelets with the same number of vanishing moments like the studies conducted by Bior, Coiflet, Symlet, and Daubechies [18]. The findings of this study are in consistence with the previous studies showing high efficiency of these mother wavelets in corrosion detection. These findings are shown in Fig. 7. It should be noted that, Daubechies mother wavelet is more sensitive to damage and leads to wavelet coefficients of greater value. Therefore, in this paper Daubechies mother wavelet is mostly used to investigate other capabilities of wavelet transform in the field of damage detection.

As shown in Figs. 6 and 7, both static profile and mode shape of the damaged beam can be used in corrosion detection, but using static profile in corrosion detection is more suitable because it can be obtained very easily in practice.

As discussed in the section 2, minimum number of vanishing moments should be determined for an accurate corrosion

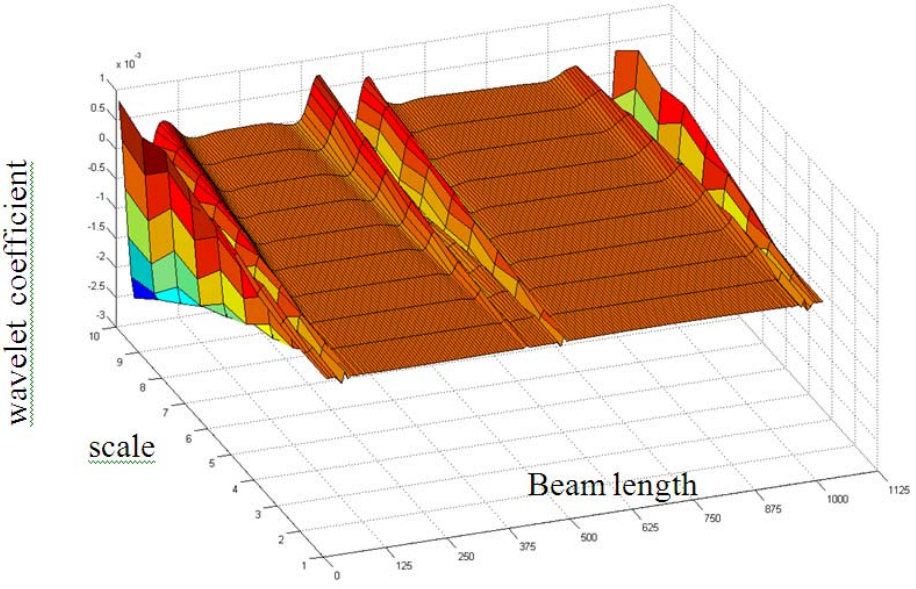


(a)

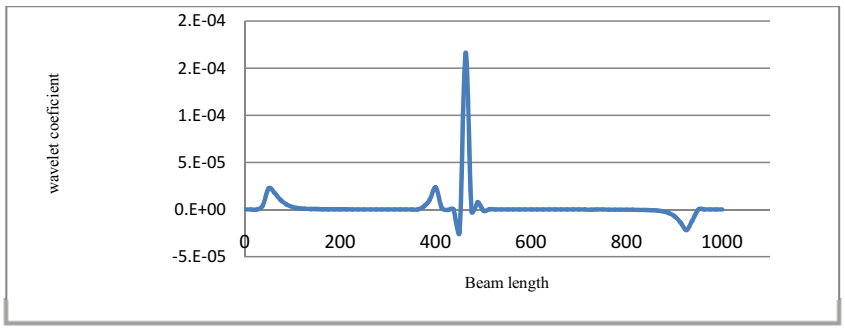


(b)

**Fig. 6** Wavelet transform of damaged beam static profile: a) CWT b) DWT

detection in damaged structures. Therefore, Daubechies mother wavelet with different number of vanishing moments is used for the wavelet analysis of mode shapes. Scenario number 9 is used in this section and the obtained results are summarized in Fig. 8. It can be concluded that in the case of corrosion detection in simply supported RC beams, wavelets with at least 4 vanishing moments should be used for accurate corrosion detection. Other Mother wavelets like Symlet, Coiflet and Bior are also used and the same results regarding the number of vanishing moments are observed.

Scenarios number 5 to 9 are used to demonstrate the capability of wavelet analysis in developing a relationship between wavelet coefficients and corrosion percentage. In each case, maximum value of continuous wavelet coefficient of damaged zone is calculated by utilizing Coiflet mother wavelet, as summarized in Fig. (9). For practical applications, a linear trend-line is best fitted to these data, as presented in Eq. (24):

$$CP = 3.33 \times 10^5 \, CW_{coif} + 666.6 \tag{24}$$

where $CW$ denotes the maximum of continuous wavelet coefficients in damaged zone, the subscript coif implies the Coiflet mother wavelet, which is used for development of this

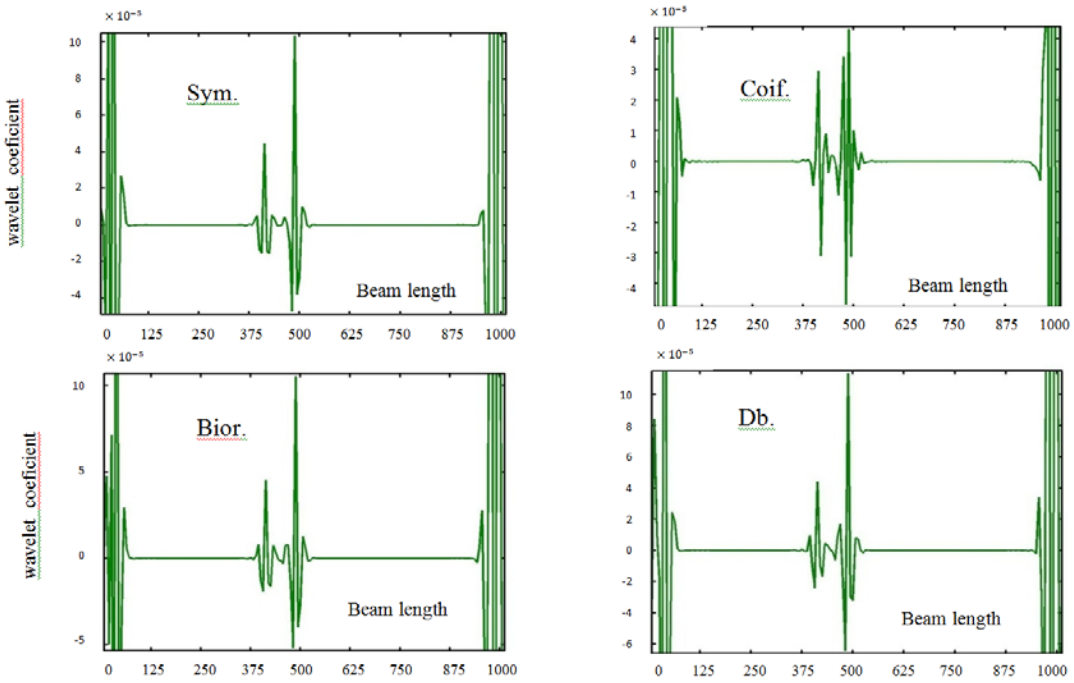


**Fig. 7** discrete wavelet transform of damaged beam first mode shape by different mother wavelets

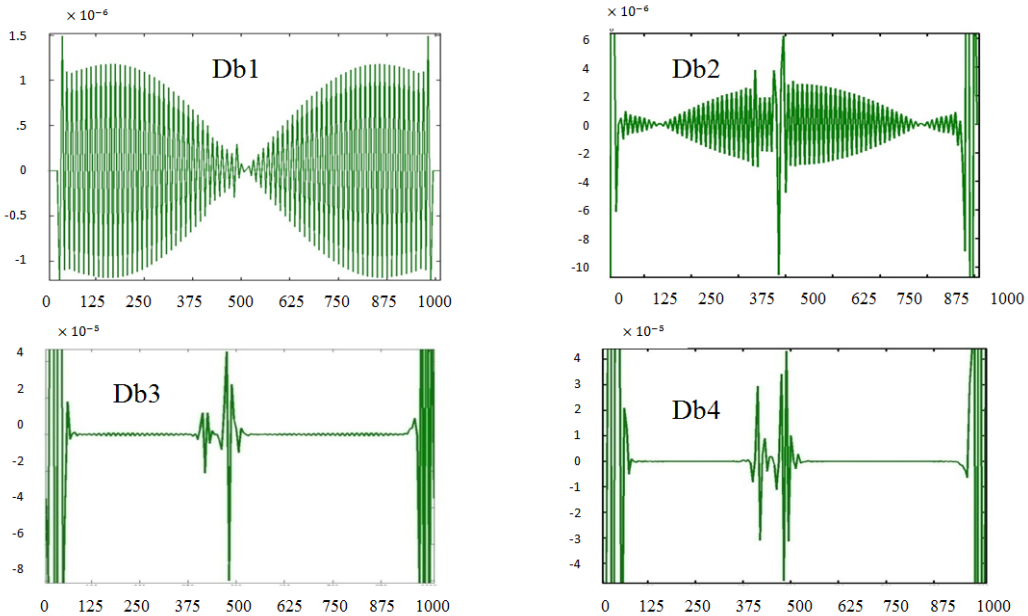


**Fig. 8** DWT results withDaubechies mother wavelet

equation and CP represents maximum corrosion percentage of damaged zone. Using other mother wavelets is also possible, but the constant values of the equation may change. Similar procedure is implemented with DWT and Eq. (25) is obtained as follows:

$$CP=3\times10^{8}\,DW_{coif}+2670 \quad (25)$$

where $DW_{coif}$ denotes the maximum of discrete wavelet coefficients of damaged zone. Therefore, implementing Eq. (24) and Eq. (25) in practical conditions, corrosion severity can be determined by performing wavelet analysis on mode shape or static profile of the damaged beam.

To verify the reliability and accurateness of the proposed equations, scenario number 15 with 7 percent of corrosion expansion is analyzed and then, its wavelet coefficient is used as an input for the presented equations. Based on Eq. (24) and Eq. (25) , the corresponding corrosion percentages of 7.2 and 7.22 percent is obtained respectively, which are reasonable.

Capability of the presented method to detect multiple damages is evaluated, considering scenarios number 10 to 14 (with two damaged locations). The three first mode shapes are extracted and analyzed. As it can be seen in Fig. 10, high efficiency of the presented method for detecting multiple damages in each mode shape can be concluded.

Eqs .(24) and (25) can also be used in cases where corrosion is occurred in more than one location. In these cases, the reinforcing beam should be divided into several parts in a

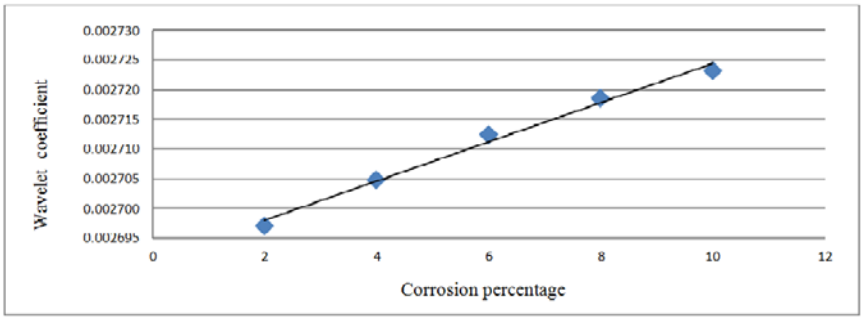


**Fig. 9** corrosion percentage vs. continuous wavelet coefficients

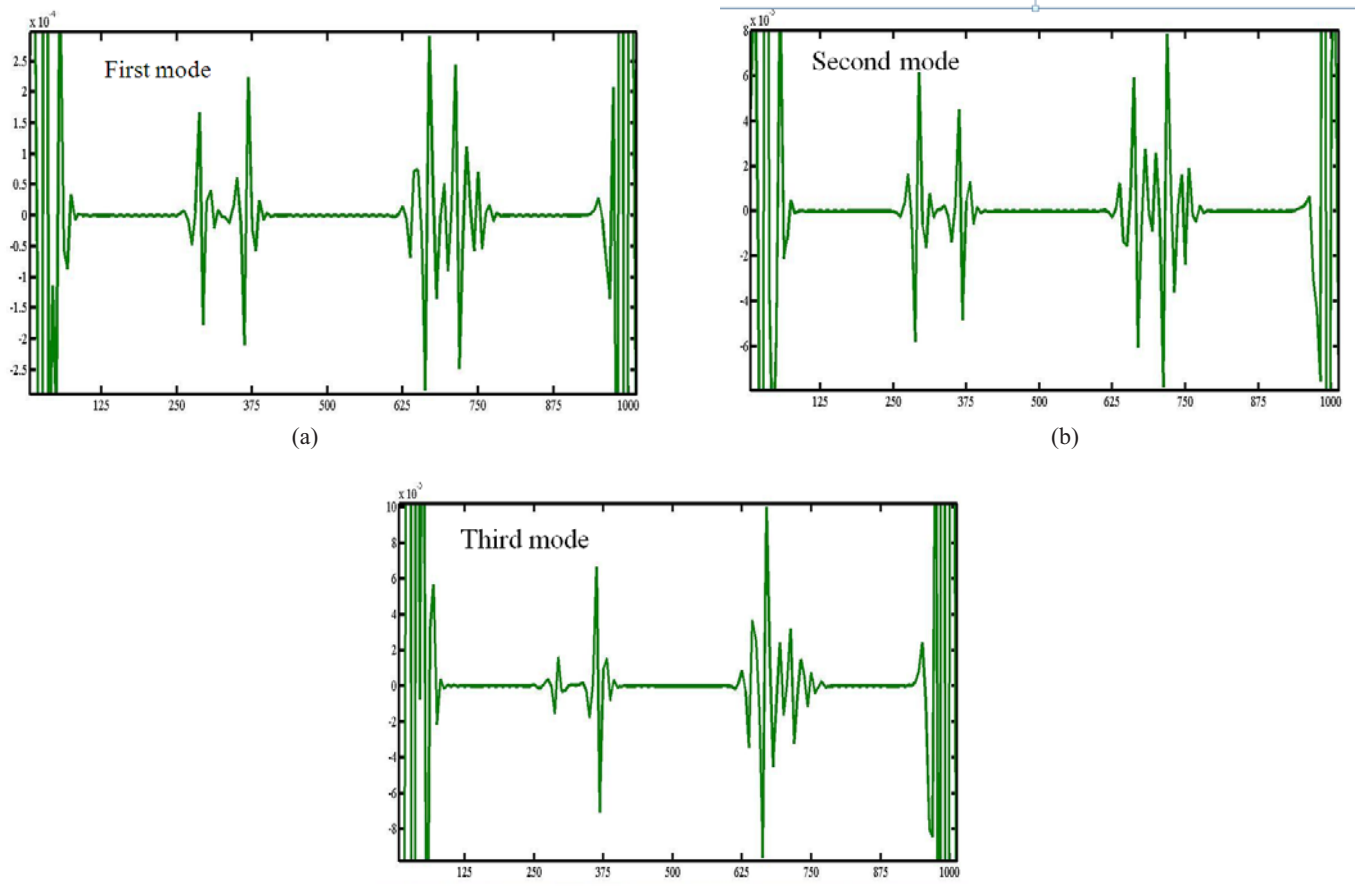


(a) (b) (c)

**Fig. 10** DWT of first three mode shapes of beam with multiple damage :a) first mode. b) second mode. c) third mode

manner that each part includes just one corrosion zone. Then, corrosion severity can be investigated in each part separately.

It should be noted that, extracting mode shapes higher than mode of order three is possible with lots of difficulties in practice, so damage detection by using lower mode shape is more suitable. Therefore, in this paper just first three mode shapes has been investigated and reasonable results are obtained. As it is apparent in Fig.10, Peak of wavelet coefficients in mode 3 has greater values than mode 1 and 2, thus if noise exist in the system because of the vehicle motion or wind, using mode shape 3 is more efficient because it is more sensitive to damage.

## 6. Conclusion

In this paper, a new method for corrosion detection in RC beams is proposed based on wavelet analysis of dynamic mode shapes and static deflection profile of damaged beams. Continuous and discrete wavelet analyses are employed. Findings of the study shows that these two wavelet transforms yield high efficiency in the detection of single and multiple corrosion zones. In addition, a relationship is developed for identifying and quantifying the corrosion severity based on wavelet coefficients. In addition, based on the results of this study, the following statements can also be concluded:

- Both discrete and continuous wavelet transforms can be used for corrosion detection, but discrete wavelet transform is suggested because of its simplicity.
- Mother wavelet type has little effect on the detection procedure, while at least 4 vanishing moments is necessary for an accurate corrosion detection.
- Results of the present study demonstrated that higher mode shapes are more sensitive to damage.

## References


[1] Bakhtiari Nejad F. , Rahai A. , Esfandiari A. Theoretical and experimental damage detection method of structures using static displacements. IJCE. 2004; 2 (2) :112-122.

[2] Farrar C.R, Jauregui D.V. Damage Detection Algorithms Applied experimental and numerical modal data from I-40 bridge. Los Alamos national laboratory report 1996; LA-13074-MS.

[3] Ratcliffe C.P. Damage detection using a modified Laplacian operator on mode shape data. Journal of Sound and Vibration 1997; 204, 505–517.

[4] Doebling S.W, Farrar C.R., Prime M.B . A summary review of vibration-based damage identification method. The Shock and Vibration Digest1998; 30, 91–105.

[5] Abbasnia R, Mirzadeh N, Kildashti K. Assessment of axial force effect on improved damage index of confined RC beam-column members. IJCE. 2011; 9 (3) :237-246.

[6] 6.West W.M . Illustration of the use of modal assurance criterion to detect structural changes in an orbiter test specimen. in proc. Air force conference on aircraft structural integrity1984;1-6.

[7] Pandey A.K , Biswas M, Samman M.M . Damage detection from changes in curvature mode shapes. Journal of Sound and Vibration1991; 145, 321–332.

[8] Staszewski W. J . Advanced data preprocessing for damage identificationbased on pattern recognition. Int. J. Syst. Sci 2000; 31_11_,1381–1396.

[9] Kijewski T, Kareem A. Wavelet transform for system identification in civil engineering. Computer-Aided Civil and Infrastructure Engineering 2003; 18 (5), 339–355.

[10] Liew K.M , Wang Q . Application of wavelet theory for crack identification in structures. Journal of Engineering Mechanics, ASCE 1998; 142 (2), 152–157.

[11] Wang Q, Deng X. Damage detection with spatial wavelets. International Journal of Solid and Structures 1999;36:3443–68.

[12] Hong J-C, Kim YY, Lee HC, Lee YW. Damage detection using Lipschitz exponent estimated by the wavelet transform: applications to vibration modes of beam. International Journal of Solid and Structures 2002;39:1803–46.

[13] Gentile A, Messina A. On the continuous wavelet transforms applied to discrete vibrational data for detecting open cracks in damaged beams. International Journal of Solid and Structures 2003; 40:295–315.

[14] Douka E, Loutridis S, Trochidis A. Crack identification in beams using wavelet analysis. International Journal of Solid and Structures 2003;40:3557–69.

[15] Wu N., Wang Q., Experimental studies on damage detection of beam structures with wavelet transform., International Journal of Engineering Science,2011;49 (3), 253–261.

[16] Ghodrati Amiri G, Asadi A. Comparison of Different Methods of wavelet and wavelet Packet Transform in Processing Ground Motion Records. IJCE. 2009; 7 (4) :248-257.

[17] Hester D., Gonzalez A., A wavelet-based damage detection algorithm based on bridge acceleration response to a vehicle, Mechanical Systems and Signal Processing,2012;28, 145–166.

[18] Hou Z, Noori M . Application of wavelet analysis for structural health monitoring. Proc., 2nd Int. Workshop on Struct. Health Monitoring, Stanford University, Stanford, Calif 1999; 946–955.

[19] Saetta A, Scotta R, Vitaliani R . Coupled environmental-mechanical damage model of RC structure. Journal of Engineering Mechanics, ASCE 1999;125(8):930–40.

[20] Lubliner J , Oliver J, Oller S, Oñate E . A Plastic-Damage Model for Concrete. International Journal of Solids and Structures1989; vol. 25, no. 3, pp. 229–326.

[21] Saetta A, Scotta R, Vitaliani R. Mechanical behaviour of concrete under physical-chemical attacks. Journal of Engineering Mechanics, ASCE 1998;124(10):1100–9.

[22] Berto L, Simoni P ,Saetta A . Numerical modelling of bond behaviour in RC structures affected by reinforcement corrosion. Engineering Structures 2008; 1375–1385.

[23] Fang C, Lundgren K, Chen L, Zhu C . Corrosion influence on bond in reinforced concrete. Cement and Concrete Research2004; 34 :2159–2167.

[24] Jankowiak T, Odygowski T. Identification of parameters of concrete damage plasticity constitutive model. Foundations of civil and environmental engineering 2006; No 6.

[25] Clough R.W. and Penzien J. Dynamics of structures. Computers & Structures, Inc2003, 1995 University Ave., A 94704, Berkeley, USA.